Brain Imaging and Behavior
https://doi.org/10.1007/s11682-020-00381-9

ORIGINAL RESEARCH

Frequency-specific altered global signal topography in drug-naïve first-episode patients with adolescent-onset schizophrenia

Xiao Wang [1,2] · Wei Liao [1,2] · Shaoqiang Han [1,2] · Jiao Li [1,2] · Yifeng Wang [1,2] · Yan Zhang [3] · Jingping Zhao [4] · Huafu Chen [1,5]

Abstract

Adolescent-onset schizophrenia (AOS) is a severe neuropsychiatric disease associated with frequency-specific abnormalities across distributed neural systems in a slow rhythm. Recently, functional magnetic resonance imaging (fMRI) studies have determined that the global signal. (GS) is an important source of the local neuronal activity in 0.01–0.1 Hz frequency band. However, it remains unknown whether the effects follow a specific spatially preferential pattern in different frequency bands in schizophrenia. To address this issue, resting-state fMRI data from 39 drug-naïve AOS patients and 31 healthy controls (HCs) were used to assess the changes in GS topography patterns in the slow-4 (0.027–0.073 Hz) and slow-5 bands (0.01–0.027 Hz). Results revealed that GS mainly affects the default mode network (DMN) in slow-4 and sensory regions in the slow-5 band respectively, and GS has a stronger driving effect in the slow-5 band. Moreover, significant frequency-by-group interaction was observed in the frontoparietal network. Compared with HCs, patients with AOS exhibited altered GS topography mainly located in the DMN. Our findings demonstrated that the influence of the GS on brain networks altered in a frequency-specific way in schizophrenia.

Keywords fMRI · Global signal · Functional connectivity · Adolescent-onset schizophrenia

Introduction

Schizophrenia is a devastating neurodevelopmental illness characterized by progressive deterioration (Thompson et al. 2001; Wang et al. 2018a). This illness co-occurs with neuronal disturbances that affect diverse cortical regions(Li et al. 2019a, 2019b; Woo et al. 2017; Yang et al. 2016), including the sensorimotor system (Berman et al. 2015) and thalamo-cortical circuit (Anticevic et al. 2014), as well as regions involved in higher-order cognitive functions (Reinen et al. 2018). Further evidence suggests that the disruption in the distributed structure is susceptible to age and drug effects during maturation in schizophrenia (Keshavan et al. 2014; Rapoport et al. 2012). Adolescents with schizophrenia (AOS) provide a unique opportunity to explore these dysfunctions because they are less affected by chronic antipsychotic medication and interaction with age-related neurodegeneration(Cannon et al. 2002; Douaud et al. 2007; Epstein et al. 2014). Many studies have focused on the disrupted distributed organization in schizophrenia via functional magnetic resonance imaging (fMRI)(Braun et al. 2018; van den Heuvel and Hulshoff Pol 2010).

Recent studies have demonstrated that the global signal (GS) contribute to the distributed structures during the task (Murray et al. 2014) and resting states(Keshavan et al. 2014). For example, Wong et al. found that caffeine can increase the GS, which affects the anticorrelation between the

✉ Huafu Chen
chenhf@uestc.edu.cn

[1] The Clinical Hospital of Chengdu Brain Science Institute, School of Life Science and Technology, University of Electronic Science and Technology of China, Chengdu 610054, People's Republic of China

[2] MOE Key Lab for Neuroinformation, High-Field Magnetic Resonance Brain Imaging Key Laboratory of Sichuan Province, University of Electronic Science and Technology of China, Chengdu 610054, People's Republic of China

[3] Key Laboratory for Mental Health of Hunan Province, Mental Health Institute, the Second Xiangya Hospital of Central South University, Changsha, China

[4] Mental Health Institute, the Second Xiangya Hospital of Central South University, 139, Middle Renmin Road, Changsha 410011, Hunan, China

[5] Radiology department of the First Affiliated Hospital, the Third Military Medical University, Chongqing 400038, China

Published online: 13 November 2020

default mode network (DMN) and task-positive network in HCs (Wong et al. 2016; Wong et al. 2013). By analysis the GS topology, Yang et al. found that the representation of the GS in association regions and sensory regions is different, and suggested the spatially specific changes may represent a disruption in basic brain functions in schizophrenia (Yang et al. 2016). Similar results were found in major depressive disorder (Zhu et al. 2018). Moreover, Wang et al. further confirmed that the influence of the GS on a distributed structure is dynamic in AOS (Wang et al. 2019). These studies suggest that GS is an important source of the neuronal activity itself and contains important clinical information on psychiatric disorders.

Moreover, fMRI studies have revealed specific relationships between distributed neural activity and frequency in HCs and schizophrenia patients (Braun et al. 2018; Meda et al. 2015). By analyzing the response to simulated tasks in different frequency bands, Sun et al. found that the regions of the visual cortex in HCs have frequency selectivity (Sun et al. 2007). Thereafter, frequency-dependent effects were found in different brain regions (Gohel and Biswal 2015), brain networks (Esposito et al. 2013), and functional hubs (Wang et al. 2018b Meanwhile, frequency-dependent changes were found in the amplitude of low-frequency oscillations(Hoptman et al. 2010; Yu et al. 2014), regional homogeneity (Yu et al. 2013) and functional connectivity (FC) density (Ji et al. 2017) in schizophrenia. Accumulating evidence suggests that considering the information of multiple frequency bands can better distinguish disease characteristics (Chen et al. 2016). However, studies about the frequency-specific characteristics of GS topography in AOS are lacking.

The current study assessed whether the altered topography of the GS in AOS is frequency specific. The FC method was used to investigate the pattern of GS in AOS patients and HCs at two frequency bands (slow-4: 0.027–0.08 Hz and slow-5: 0.01–0.027 Hz). Two-way analysis of covariance (ANCOVA) was used for statistical analysis. Furthermore, the relationship between the aberrance and clinical symptoms was investigated to test the contributions of frequency-specific alterations to the clinicopathology of AOS.

Materials and methods

Participants

A total of 39 first-episode patients with AOS and 31 healthy volunteers were recruited from the Second Affiliated Hospital of Xinxiang Medical University. All participants were aged from 12 years to 18 years, right-handed Han Chinese, and had received more than 6 years of formal education. The exclusion criteria for all participants were as follows: (1) any past or current neurological disorders or family history of hereditary neurological disorders; (2) history of head injury with loss of consciousness; (3) alcohol or substance abuse; (4) claustrophobia; (5) and MRI contraindications. Patients need to fulfill the following inclusion criteria: (1) DSM-IV-TR criteria for schizophrenia (Diagnostic and Statistical Manual of Mental Disorders, fourth edition text revision, American Psychiatric Association, 2000) (Zheng et al. 2015) using the Kiddie Schedule for Affective Disorders and Schizophrenia (Kaufman et al. 1997); (2) no co-morbid Axis I diagnosis; (3) duration of illness less than 2 years (Green and Schildkraut 1995; Ram et al. 1992); (4) and no current or previous antipsychotic medication. The clinical symptoms were independently assessed by two experienced psychiatrists using DSM-VI based structured interviews (SCID-I/Patient version) (First et al. 1995; Kyriakopoulos et al. 2008). To validate the initial diagnosis, we reassessed all patients 6 months after the initial diagnostic interview. The clinical negative symptomatology was further evaluated using the Positive and Negative Syndrome Scale (PANSS) (Kay et al. 1987). The fMRI data and clinical scales were collected after the initial diagnosis and before the treatment.

The study was approved by the Ethics Committee of the Second Affiliated Hospital of Xinxiang Medical University, and all participants provided written informed consent with the consent of their guardians before participating in our experiment.

Neuroimaging data acquisition

All subjects were instructed to rest with their eyes closed, not to think of anything in particular, and not to fall asleep during the scan (Duan et al. 2020; Fan et al. 2020). fMRI data were acquired on a 3 Tesla MRI system (Vision; Siemens MAGNETOM Verio, Erlangen, Germany) equipped with a high-speed gradient coil. The following parameters were used for high resolution T1-weighted volumetric 3D images: repetition time/echo time (TR/TE) = 2530/2.43 ms, matrix = 256 × 256, flip angle = 7°, voxel size = 1 × 1 × 1 mm^3 and 158 slices without inter-slice gap. At the same locations as those of the anatomical slices, the functional images were collected transversely using an echo-planar imaging (EPI) sequence with the following settings: TR/TE = 2000 ms/30 ms, flipangle = 90°33 slices, 64 × 64 matrix, 90° flip angle, field of view = 220 × 220 mm^2, interslice gap = 0.6 mm, and voxel size = 3.44×3.44×4 mm^3**Error! Digit expected.**. For each subject, 240 functional volumes were obtained.

Neuroimaging preprocessing

T1 images were segmented into WM, gray matter (GM), and cerebrospinal fluid using the DARTEL algorithm in the DPARSF toolbox. Then, the GM mask of each subject is

resampled to 3 × 3 x 3mm^3 to ensure that all bold images on both scanners are interpolated to the same resolution.

Preprocessing followed prior works (Ji et al. 2017; Power et al. 2014) and was conducted using the SPM8 toolbox. The initial 10 images were discarded (Wang et al. 2019). Images were then realigned and corrected for slice timing differences. Next, the functional images were normalized to Montreal Neurological Institute (MNI) template (voxel size: 3 mm × 3 mm × 3 mm). Notably, in the regression step, we used multiple regression to model the time-varying BOLD signal in each voxel, including the Friston 24 motion parameters, cerebrospinal, and white matter signals. The GS was excluded from the multiple regression model. The resulting images were linearly detrended and filtered using a typical bandpass, including the slow-5 bandpass (0.01–0.027 Hz) and slow-4 bandpass (0.027–0.073 Hz) (Gohel and Biswal 2015). Given that resting-state FC is sensitive to minor head movements, we calculated the mean frame-wise displacement (FD) to further determine the comparability of head movement across groups. Subsequently, the 'bad' time points, as well as their 1-back and 2-forward time points, were removed from the time series by employing a 'scrubbing' method with an FD threshold of 0.5 mm (Power et al. 2012).

Imaging data of four AOS patients and one healthy participant were excluded due to large head motion (> 2 mm translation or > 2° rotation), leaving a total of 35 AOS patients and 30 HCs for the final analysis. Importantly, AOS and HCs did not differ in the remaining time points (HC: 227.8±6.98; AOS: 225.1 ± 6.72; mean ± SD, $p = 0.09$) and mean FD (HC: 0.09 ± 0.05 AOS: 0.01 ± 0.03; mean ± SD, $p = 0.33$) after the "scrubbing".

Global gray matter signal topography calculation

The GS topography was measured by using the FC method (pairwise correlation between the GS time course and each voxel time course) (Schölvinck et al. 2010). The GS time series for each subject was acquired by calculating the mean preprocessed BOLD signal overall gray matter voxels for each time point, explicitly excluding ventricles and white matter signal(Wang et al. 2019; Yang et al. 2016; Yang et al. 2014). The correlation coefficients were then converted to z-values using Fisher's r-to-z transformation. In this work, the z-value map is referred to as the topography of GS(Aguirre et al. 1997; Fox et al. 2009).

Statistical analyses

For each pattern, one-sample t test was performed for each group. The significance level was set at $p < 0.05$ (Gaussian random field (GRF) corrected). Then, ANCOVA was conducted in SPM8 with diagnosis (two levels: AOS and HC) as a group factor and frequency band (two levels: slow-4 and slow-5) as a within-subject factor, and with age, gender and FD as covariates. GRF correction was used for cluster-level multiple comparisons correction (voxel significance $p < 0.001$, cluster significance: $p < 0.05$, corrected) (Duan et al. 2012; Li et al. 2016). Post-hoc, two-sample tests were used on clusters that showed a significant effect of group and band.

Brain regions that showed significant interaction effects were considered regions of interest (ROIs) for the following analyses. ROIs were defined as 4 mm radius spheres with the centre at the peak position of statistical differences. Finally, Spearman rho correlation was calculated between the FC in the regions that showed interaction effects and PANSS scores.

Results

Demographics and clinical symptoms

AOS and HC did not differ in gender, age, and years of education (Table 1).

Frequency-specific spatial localization of the GS

We first examined the frequency-specific spatial pattern of the GS representation in AOS and HC groups. Then, we computed voxel-wise correlations to the GS according to earlier works (Fox et al. 2009). Strikingly, non-uniform representation of the GS was observed across the brain. The topography of the GS in both groups showed significant frequency dependence (one-sample t test, GRF corrected $p < 0.05$) (Fig. 1).

Table 1 Demographic and clinical characteristics

Demographics, Mean (SD)	AOS $N = 35$	Control $N = 30$	P value
Age(year)	15.5 (1.8)	15.3 (1.6)	0.57[a]
Gender(male/female)	20/15	13/17	0.27[b]
Education (years)	8.5 (1.48)	8.7 (1.42)	0.605[a]
Duration of psychosis(months)	6.6 (6.4)	—	—
Handedness (right/left)	35/0	30/0	—
PANSS Positive Symptoms	20.42 (5.72)	—	—
PANSS Negative Symptoms	20.91 (8.41)	—	—
PANSS General Symptoms	33.28 (6.69)	—	—
PANSS Total Symptoms	74.62 (10.61)	—	—

P^a-value was obtained by two-sample t-test.

P^b-value was obtained by χ^2 two-tailed test.

Table 2 Interaction between the frequency band and group factors revealed by two-way ANCOVA

Brain areas		L/R	Cluster size	F-value	Peak coordinate		
			voxels		X	Y	Z
AOS > HC	Inferior frontal gyrus, opercular	L	54	12.31	−48	9	25
	Middle frontal gyrus	L	37	11.09	−30	24	60

The statistical significance level is corrected for multiple comparisons using GRF correction with (voxel significant $p < 0.001$, cluster significant $p < 0.05$). The peak coordinate is defined in MNI space. AOS, adolescent-onset schizophrenia; HC, healthy controls; ANCOVA, analysis of covariance; L, left; R, right; MNI, Montreal Neurological Institute.

Interaction effect between the frequency band and group

Remarkable frequency-by-group interaction effects were found in the opercular part of the left inferior frontal gyrus ($F_{(1,124)} = 12.31$) and left middle frontal gyrus ($F_{(1,124)} = 11.09$) (Fig. 2, A). Post-hoc analysis revealed that FC in the regions shown interaction effects were significantly lower in the slow-5 band in AOS patients, but no significant effect was detected in the slow-4 band (Fig. 2, B).

Main effect of the frequency band

We examined the effect of frequency band on the topography of GS. The brain regions that showed a significant main effect of frequency band were mainly located in the left inferior temporal gyrus ($F_{(1,124)} = 39.60$), right superior temporal gyrus ($F_{(1,124)} = 51.46$), right middle frontal gyrus ($F_{(1,124)} = 26.48$), orbital part of the left inferior frontal gyrus ($F_{(1,124)} = 29.24$), left precuneus ($F_{(1,124)} = 46.45$), right lingual gyrus ($F_{(1,124)} = 17.92$), and left cerebellar crus 1($F_{(1,124)} = 34.71$) (Fig. 3, A). Post-hoc analysis revealed that the FC in the slow-4 band was lower than that in the slow-5 band (Table 3).

Main effect of the group

The main effect of the group was observed in the left superior frontal gyrus, orbital part ($F_{(1,124)} = 18.32$), right middle temporal gyrus ($F_{(1,124)} = 22.07$) and right precuneus ($F_{(1,124)} = 15.38$) (Fig. 3, B). Post-hoc analysis revealed that the AOS patients showed significantly higher FC in the orbital frontal cortex but lower FC in the middle temporal gyrus and precuneus compared with the HCs (Table 4).

Correlation with clinical symptoms

No significant correlation was found between the altered FC and PANSS scores in AOS.

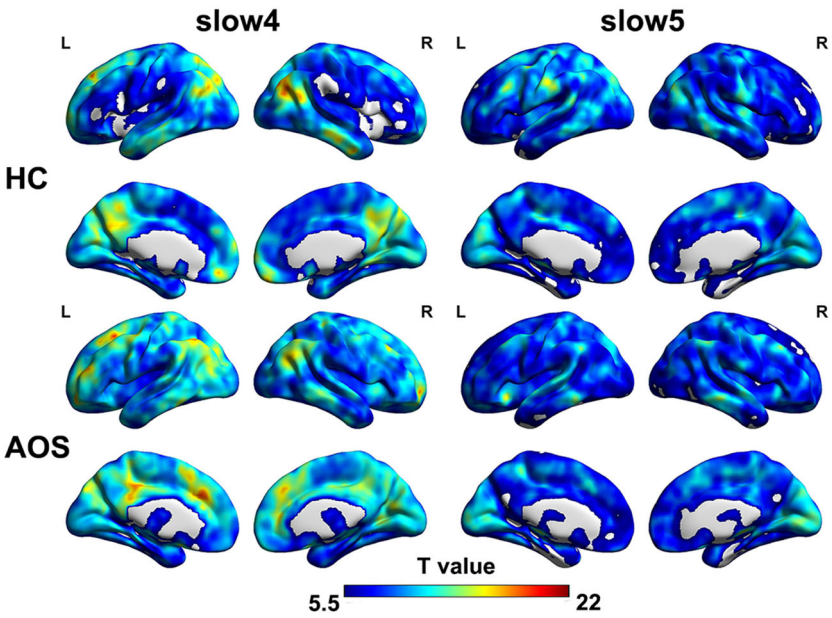

Fig. 1 Frequency-specific spatial localization of the GS for AOS and HC groups. One-sample t tests were performed for each group in different frequency bands. The significance level was set at $p < 0.05$ (GRF Corrected)

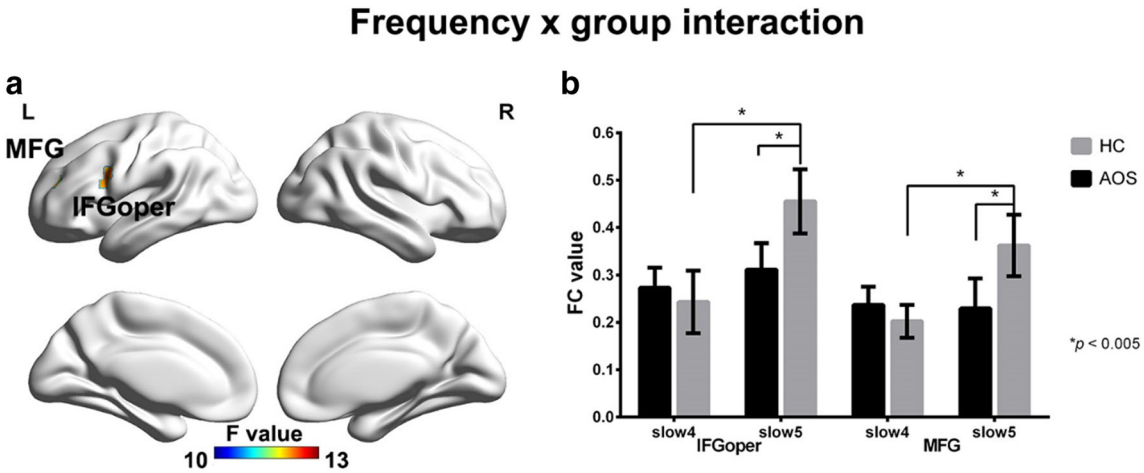

Fig. 2 The interaction between the frequency band and group (Fig. 2A). The results were obtained by two-way ANCOVA and post-hoc test. We found decreased FC in patients with AOS in the slow-5 band. No significant difference in FC was observed between the groups in the slow-4 band (Fig. 2B). FC, functional connectivity; AOS, adolescent-onset schizophrenia; HC, healthy control (Table 2)

Discussion

In this study, we used the FC method to investigate the changes in the GS topography in AOS patients at two frequency bands (slow-4 and slow-5). The representation of GS is frequency-specific, mainly affect the DMN in the slow-4 band and the sensory network in the slow5. Moreover, significant frequency-by-group interaction was observed in the opercular part of the left inferior frontal gyrus and left middle frontal gyrus. Besides, patients with AOS demonstrated impaired GS topography mainly in the DMN. Our findings offered initial evidence that the effect of GS on different networks is frequency-specific, and the effect is altered in patients with AOS.

Frequency-specific GS topography within group

The current work showed a generally positive correlation between the GS and voxel-wise BOLD signals in the brain's gray matter in the slow-4 and slow-5 bands. In line with a previous study, the topography of the GS in different frequency bands was indeed nonuniform and different (Yang et al. 2016). In the HC group, the GS topography was mainly in the DMN and the inferior temporal gyrus in the slow-4 band, while mainly in the sensory regions, visual network, and frontoparietal network in the slow-5 band. In the AOS group, the GS topography showed similar results but the distribution was blurred. The current results were consistent with the previous study that the DMN emerged from the low rhythmic mechanism and concentrated within ultra-low frequency,

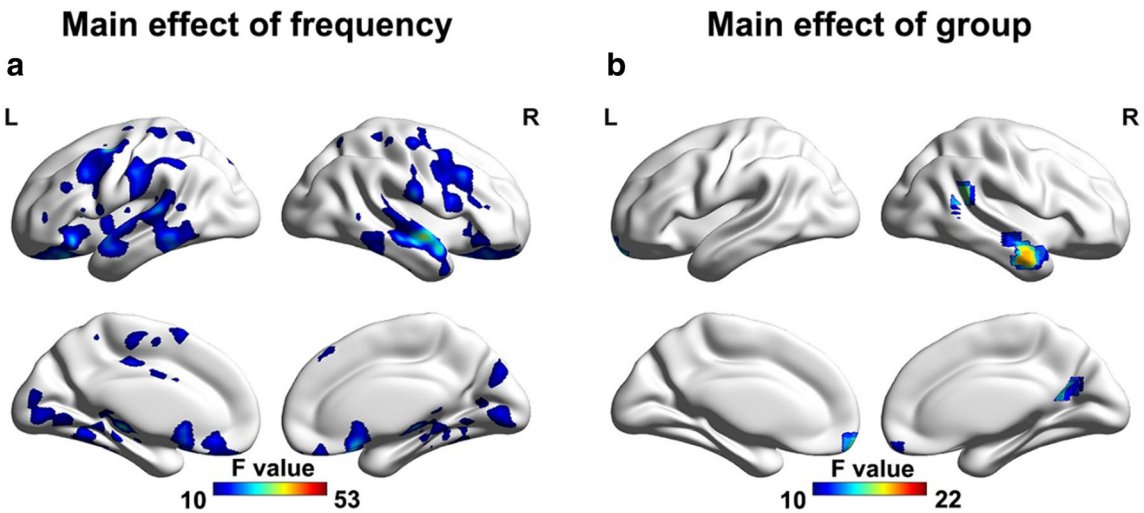

Fig. 3 The main effect of the frequency band factor. Statistical significance level is corrected for multiple comparisons using GRF correction (voxel significance $p < 0.001$, cluster significance: $p < 0.05$, corrected)

Table 3 The main effect of the frequency band revealed by two-way ANCOVA

Brain region		L/R	Cluster size	F-value	Peak coordinate		
			voxels		X	Y	Z
slow4 < slow5	Inferior temporal gyrus	L	235	39.60	−47	−37	−26
	Superior temporal gyrus	R	125	51.46	57	0	−11
	Middle frontal gyrus	R	121	26.28	48	18	39
	Inferior frontal gyrus, orbital	L	160	29.24	−20	25	−22
	Precuneus	L	141	46.45	−3	−60	69
	Lingual gyrus	L	320	17.92	−21	−49	−9
	Cerebellar crus 1	L	101	34.71	−24	−36	−57

The statistical significance level is corrected for multiple comparisons using GRF correction with (voxel significant $p < 0.001$, cluster significant $p < 0.05$). The peak coordinate is defined in MNI space. AOS, adolescent-onset schizophrenia; HC, healthy controls; ANCOVA, analysis of covariance; L, left; R, right; MNI, Montreal Neurological Institute.

mainly in the slow-4 band (Gohel and Biswal 2015; Li et al. 2015; Wu et al. 2008). Moreover, the spectral features of visual and sensorimotor systems were similar and showed consistency of synchronization with the GS (Wu et al. 2008). The distinct patterns of the GS topography across the frequency bands may be due to the natural frequency required for the distinct brain regions in processing time-locked incoming external stimuli versus internal maintenance and representation of parallel information (Buzsáki and Draguhn 2004; Yang et al. 2016). These results uncovered the underling disruption of neuronal signals in different frequency bands in schizophrenia.

Frequency-dependent changes in the GS topography in AOS

In patients with AOS, the GS topography is influenced by the interaction between frequency band and disease. In particular, the GS topography was significantly lower in the slow-5 band but did not change significantly in the slow-4 band in the AOS patients. Although the physiological mechanisms of slow-4 and slow-5 bands remain unclear, many neuroimaging studies have found that the abnormalities in schizophrenia are frequency sensitive(Thompson and Fransson 2015; Yu et al. 2014; Yu et al. 2013). For example, by using fMRI, Zuo et al. found that different network activities have their own unique frequencies in schizophrenia (Zuo et al. 2010). Moreover, Markus et.al proposed that frequency-specific neuronal correlations in large-scale cortical networks may be 'fingerprints' of canonical neuronal computations underlying cognitive processes(Siegel et al. 2012). Further evidence confirmed the presence of abnormal interaction between disease and frequency in patients with schizophrenia (Meda et al. 2015; Mingoia et al. 2013; Yu et al. 2014). The current findings demonstrated that the abnormal GS topography in AOS was mainly in the slow-5 band. Compared with the slow-4 band, the slow-5 had a higher power and was more dominant within the cerebral cortex(Han et al. 2011). However, the FC in the slow-5 band was mainly localized within the subcortical and sensory regions (Ji et al. 2017; Wu et al. 2008; Wu et al. 2016). In the AOS patients, nonspecific sensory and motor neurological abnormalities were frequently reported, and these abnormalities further affected disease development during subsequent maturation (Hong et al. 2008; Kumperscak 2011). Our results were consistent with the previous hypothesis that, each cortical area tended to preserve its own natural frequency even when damaged (Rosanova et al. 2009).

Moreover, the area of the frontal lobe that exhibited interaction effect was mainly in the junction between the frontal gyrus and the parietal lobe. The frontoparietal network allows

Table 4 The main effect of the group revealed by two-way ANCOVA

Brain region		L/R	Cluster size	F-value	Peak coordinate		
			voxels		X	Y	Z
AOS > HC	Superior frontal gyrus, orbital	L	48	18.32	−8	56	−14
AOS < HC	Middle temporal gyrus	R	79	22.07	56	−4	−21
	Precuneus	R	37	15.38	12	−56	20

The statistical significance level is corrected for multiple comparisons using GRF correction with (voxel significant $p < 0.001$, cluster significant $p < 0.05$). The peak coordinate is defined in MNI space. AOS, adolescent-onset schizophrenia; HC, healthy controls; ANCOVA, analysis of covariance; L, left; R, right; MNI, Montreal Neurological Institute.

an individual to understand the action of others 'from the inside' and gives the observer a first-person grasp of the motor goals and intentions of other individuals (Rizzolatti and Sinigaglia 2010; Zhang et al. 2019). Our results demonstrate that the GS topography is frequency-specific in AOS and may reflect the neuropathological mechanisms of the disruption in gating information flow within the brain in schizophrenia.

Difference in the GS topography between groups

The spatial pattern of the GS representation was different between the AOS and HC groups. AOS patients exhibited increased FC in the superior frontal gyrus, orbital part, and decreased FC in the middle temporal gyrus and precuneus relative to HCs. Our results indicate that the influence of the GS on the DMN is changed in AOS. It is consistent with previous studies that functional connectivity of the DMN is disrupted in schizophrenia (Liao et al. 2018; Tang et al. 2013; van den Heuvel and Fornito 2014; Wang et al. 2017). Moreover, the DMN has been demonstrated to comprise multiple, dissociated components (Andrews-Hanna et al. 2010). The abnormalities of the DMN vary from the component to component in schizophrenia (Du et al. 2015; Hu et al. 2017). The current findings support the hypothesis that the subsystem of the DMN is altered in schizophrenia.

Limitation

The limitation of the current study should be considered. The size of the sample in the current study is relatively small. However, such a sample is feasible compared with the incidence of AOS. Second, in the process of data collection, we arranged the subjects to keep their eyes closed. Although a series of measures were taken to ensure that the subjects did not fall asleep, it is still a matter need to concern. We will refine our design in future studies. Third, in the current study, we chose a mild GRF theory for multiple comparison correction rather than the false discovery rate (FDR) correction, which makes the current findings to be considered as preliminary.

Conclusion

In this study, we investigated the spatial distribution of the GS across the brain in AOS patients at specific frequency band. This examination uncovered a strikingly frequency-dependent relationship in GS representation in many brain regions. Specially, regions with significant interaction mainly involved the frontoparietal network. Furthermore, the influence of the GS on the subsystem of the DMN is demonstrated altered in AOS. Our observations demonstrate that the GS topography in AOS is frequency-dependent and provide potential implications for exploring schizophrenia.

Funding information This research was supported by the National Key Project of Research and Development of Ministry of Science and Technology (2018AAA0100705), the Natural Science Foundation of China (61,533,006, u1808204, 61,806,042 and 61,673,089), and the Sichuan Science and Technology Program(2018TJPT0016 and 2019YJ0180).

Compliance with ethical standards

Conflict of interest The authors declare no conflict of interest.

Ethical approval All procedures performed were following the ethical standards of the institutional and/or national research committee and with the 1964 Helsinki Declaration and its later amendments or comparable ethical standards.

Informed consent Informed consent was obtained from all individual participants included in the study.

References

Aguirre, G. K., Zarahn, E., & D'Esposito, M. (1997). Empirical analyses of BOLD fMRI statistics. II. Spatially smoothed data collected under null-hypothesis and experimental conditions. *Neuroimage, 5*(3), 199–212. https://doi.org/10.1006/nimg.1997.0264.

Andrews-Hanna, J. R., Reidler, J. S., Sepulcre, J., Poulin, R., & Buckner, R. L. (2010). Functional-anatomic fractionation of the brain's default network. *Neuron, 65*(4), 550–562. https://doi.org/10.1016/j.neuron.2010.02.005.

Anticevic, A., Cole, M. W., Repovs, G., Murray, J. D., Brumbaugh, M. S., Winkler, A. M., & Glahn, D. C. (2014). Characterizing Thalamo-Cortical Disturbances in Schizophrenia and Bipolar Illness. *Cerebral Cortex, 24*(12), 3116–3130. https://doi.org/10.1093/cercor/bht165.

Berman, R. A., Gotts, S. J., Mcadams, H. M., Greenstein, D., Lalonde, F., Clasen, L., & Raznahan, A. (2015). Disrupted sensorimotor and social–cognitive networks underlie symptoms in childhood-onset schizophrenia. *Brain A Journal of Neurology, 139*(Pt 1), 276. https://doi.org/10.1093/brain/awv306.

Braun, U., Schaefer, A., Betzel, R. F., Tost, H., Meyer-Lindenberg, A., & Bassett, D. S. (2018). From Maps to Multi-dimensional Network Mechanisms of Mental Disorders. *Neuron, 97*(1), 14–31. https://doi.org/10.1016/j.neuron.2017.11.007.

Buzsáki, G., & Draguhn, A. (2004). *Neuronal Oscillations in Cortical Networks. Science, 304*(5679), 1926. https://doi.org/10.1126/science.1099745.

Cannon, M., Caspi, A., Moffitt, T. E., Harrington, H. L., Taylor, A., Murray, R. M., & Poulton, R. (2002). Evidence for Early-Childhood, Pan-Developmental Impairment Specific to Schizophreniform Disorder: Results From a Longitudinal Birth Cohort. *Archives of General Psychiatry, 59*(5), 449–456. https://doi.org/10.1001/archpsyc.59.5.449.

Chen, H., Duan, X., Liu, F., Lu, F., Ma, X., Zhang, Y., & Chen, H. (2016). Multivariate classification of autism spectrum disorder using frequency-specific resting-state functional connectivity–A multi-center study. *Progress in Neuro-Psychopharmacology and Biological Psychiatry, 64*, 1–9. https://doi.org/10.1016/j.pnpbp.2015.06.014.

Douaud, G., Smith, S., Jenkinson, M., Behrens, T., Johansenberg, H., Vickers, J., & Matthews, P. M. (2007). Anatomically related grey and white matter abnormalities in adolescent-onset schizophrenia. *Brain, 130*(Pt 9), 2375–2386. https://doi.org/10.1093/brain/awm184.

Du, Y., Pearlson, G. D., Yu, Q., He, H., & Calhoun, V. D. (2015). Interaction among subsystems within default mode network diminished in schizophrenia patients: A dynamic connectivity approach. *Schizophrenia Research, 170*(1), 55–65. https://doi.org/10.1016/j.schres.2015.11.021.

Duan, X., He, S., Liao, W., Liang, D., Qiu, L., Wei, L., & Chen, H. (2012). Reduced caudate volume and enhanced striatal-DMN integration in chess experts. *Neuroimage, 60*(2), 1280–1286. https://doi.org/10.1016/10.1016/j.neuroimage.2012.01.047.

Duan, X., Hu, M., Huang, X., Su, C., Zong, X., Dong, X., & Chen, H. (2020). Effect of Risperidone Monotherapy on Dynamic Functional Connectivity of Insular Subdivisions in Treatment-Naive, First-Episode Schizophrenia. *Schizophr Bull, 46*(3), 650–660. https://doi.org/10.1093/schbul/sbz087.

Epstein, K. A., Cullen, K. R., Mueller, B. A., Robinson, P., Lee, S., & Kumra, S. (2014). White matter abnormalities and cognitive impairment in early-onset schizophrenia-spectrum disorders. *Journal of the American Academy of Child & Adolescent Psychiatry, 53*(3), 362–372. https://doi.org/10.1016/j.jaac.2013.12.007.

Esposito, F., Tessitore, A., Giordano, A., De Micco, R., Paccone, A., Conforti, R., Tedeschi, G. (2013). Rhythm-specific modulation of the sensorimotor network in drug-naive patients with Parkinson's disease by levodopa. Brain, 136(Pt 3), 710–725. https://doi.org/10.1093/brain/awt007

Fan, Y.-S., Li, Z., Duan, X., Xiao, J., Guo, X., Han, S., & Chen, H. (2020). Impaired interactions among white-matter functional networks in antipsychotic-naive first-episode schizophrenia. *Human Brain Mapping, 41*(1), 230–240. https://doi.org/10.1002/hbm.24801.

First, M. B., Spitzer, R. L., Gibbon, M., & Williams, J. B. W. (1995). The Structured Clinical Interview for DSM-III-R Personality Disorders (SCID-II). Part I: Description. Journal of Personality Disorders.

Fox, M. D., Zhang, D., Snyder, A. Z., & Raichle, M. E. (2009). The global signal and observed anticorrelated resting state brain networks. *Journal of Neurophysiology, 101*(6), 3270–3283. https://doi.org/10.1152/jn.90777.2008.

Gohel, S. R., & Biswal, B. B. (2015). Functional integration between brain regions at rest occurs in multiple-frequency bands. *Brain Connect, 5*(1), 23–34. https://doi.org/10.1089/brain.2013.0210.

Green, A. I., & Schildkraut, J. J. (1995). Should Clozapine Be a First-line Treatment for Schizophrenia? The Rationale for a Double-Blind Clinical Trial in First-Episode Patients. *Harvard Review of Psychiatry, 3*(1), 1–9. https://doi.org/10.3109/10673229509017159.

Han, Y., Wang, J., Zhao, Z., Min, B., Lu, J., Li, K., & Jia, J. (2011). Frequency-dependent changes in the amplitude of low-frequency fluctuations in amnestic mild cognitive impairment: a resting-state fMRI study. *Neuroimage, 55*(1), 287–295. https://doi.org/10.1016/j.neuroimage.2010.11.059.

Hong, L. E., Summerfelt, A., Mitchell, B. D., Mcmahon, R. P., Wonodi, I., Buchanan, R. W., & Thaker, G. K. (2008). Sensory Gating Endophenotype Based on Its Neural Oscillatory Pattern and Heritability Estimate. *Archives of General Psychiatry, 65*(9), 1008. https://doi.org/10.1001/archpsyc.65.9.1008.

Hoptman, M. J., Zuo, X. N., Butler, P. D., Javitt, D. C., D'Angelo, D., Mauro, C. J., & Milham, M. P. (2010). Amplitude of low-frequency oscillations in schizophrenia: A resting state fMRI study. *Schizophrenia Research, 117*(1), 13–20. https://doi.org/10.1016/j.schres.2009.09.030.

Hu, M. L., Zong, X. F., Mann, J. J., Zheng, J. J., Liao, Y. H., Li, Z. C., . . . Tang, J. S. (2017). A Review of the Functional and Anatomical Default Mode Network in Schizophrenia. Neurosci Bull, 33(1), 73–84. https://doi.org/10.1007/s12264-016-0090-1

Ji, G.-J., Liao, W., Chen, F.-F., Zhang, L., & Wang, K. (2017). Low-frequency blood oxygen level-dependent fluctuations in the brain white matter: more than just noise. *Scientific Bulletin, 62*, 656–657. https://doi.org/10.1016/j.scib.2017.03.021.

Kaufman, J., Birmaher, B., Brent, D., Rao, U., Flynn, C., Moreci, P., . . . Ryan, N. (1997). Schedule for Affective Disorders and Schizophrenia for School-Age Children-Present and Lifetime Version (K-SADS-PL): initial reliability and validity data. J Am Acad Child Adolesc Psychiatry, 36(7), 980–988. https://doi.org/10.1097/00004583-199707000-00021

Kay, S. R., Fiszbein, A., & Opler, L. A. (1987). The positive and negative syndrome scale (PANSS) for schizophrenia. *Schizophrenia Bulletin, 13*(2), 261. https://doi.org/10.1093/schbul/13.2.261.

Keshavan, M. S., Giedd, J., Lau, J. Y., Lewis, D. A., & Paus, T. (2014). Changes in the adolescent brain and the pathophysiology of psychotic disorders. *Lancet Psychiatry, 1*(7), 549–558. https://doi.org/10.1016/S2215-0366(14)00081-9.

Kumperscak, H. G. (2011). Psychiatric Disorders – Trends and Developments (Vol. 6): InTech.

Kyriakopoulos, M., Vyas, N. S., Barker, G. J., Chitnis, X. A., & Frangou, S. (2008). A diffusion tensor imaging study of white matter in early-onset schizophrenia. *Biol Psychiatry, 63*(5), 519–523. https://doi.org/10.1016/j.biopsych.2007.05.021.

Li, F., Lui, S., Yao, L., Hu, J., Lv, P., Huang, X., & Gong, Q. (2016). Longitudinal Changes in Resting-State Cerebral Activity in Patients with First-Episode Schizophrenia: A 1-Year Follow-up Functional MR Imaging Study. *Radiology, 279*(3), 151334. https://doi.org/10.1148/radiol.2015151334.

Li, J. M., Bentley, W. J., & Snyder, L. H. (2015). Functional connectivity arises from a slow rhythmic mechanism. *Proc Natl Acad Sci U S A, 112*(19), 2527–2535. https://doi.org/10.1073/pnas.1419837112.

Li, M., Becker, B., Zheng, J., Zhang, Y., Chen, H., Liao, W., et al. (2019a). Dysregulated Maturation of the Functional Connectome in Antipsychotic-Naive, First-Episode Patients With Adolescent-Onset Schizophrenia. *Schizophr Bull, 45*(3), 689–697. https://doi.org/10.1093/schbul/sby063.

Li, M., Wang, D., Ren, J., Langs, G., Stoecklein, S., Brennan, B. P., et al. (2019b). Performing group-level functional image analyses based on homologous functional regions mapped in individuals. *PLoS Biol, 17*(3), e2007032. https://doi.org/10.1371/journal.pbio.2007032.

Liao, W., Fan, Y.-S., Yang, S., Li, J., Duan, X., Cui, Q., & Chen, H. (2018). Preservation Effect: Cigarette Smoking Acts on the Dynamic of Influences Among Unifying Neuropsychiatric Triple Networks in Schizophrenia. *Schizophrenia Bulletin, 45*(6), 1242–1250. https://doi.org/10.1093/schbul/sby184.

Meda, S. A., Zheng, W., Ivleva, E. I., Poudyal, G., Keshavan, M. S., Tamminga, C. A., .Calhoun, V. D. (2015). Frequency-Specific Neural Signatures of Spontaneous Low-Frequency Resting State Fluctuations in Psychosis: Evidence From Bipolar-Schizophrenia Network on Intermediate Phenotypes (B-SNIP) Consortium. Schizophrenia Bulletin, 41(6). https://doi.org/10.1093/schbul/sbv064

Mingoia, G., Langbein, K., Dietzek, M., Wagner, G., Smesny, S., Scherpiet, S., & Gaser, C. (2013). Frequency domains of resting state default mode network activity in schizophrenia. *Psychiatry Research, 214*(1), 80–82. https://doi.org/10.1016/j.pscychresns.2013.05.013.

Murray, J. D., Anticevic, A., Gancsos, M., Ichinose, M., Corlett, P. R., Krystal, J. H., & Wang, X. J. (2014). Linking Microcircuit Dysfunction to Cognitive Impairment: Effects of Disinhibition Associated with Schizophrenia in a Cortical Working Memory Model. *Cerebral Cortex, 24*(4), 859–872. https://doi.org/10.1093/cercor/bhs370.

Sun, P., Ueno, K., Waggoner, R. A., Gardner, J. L., Tanaka, K., & Cheng, K. (2007). A temporal frequency-dependent functional architecture in human V1 revealed by high-resolution fMRI. *Nature Neuroscience, 10*(11), 1404–1406. https://doi.org/10.1038/nn1983.

Power, J. D., Barnes, K. A., Snyder, A. Z., Schlaggar, B. L., & Petersen, S. E. (2012). Spurious but systematic correlations in functional connectivity MRI networks arise from subject motion. *Neuroimage, 59*(3), 2142–2154. https://doi.org/10.1016/j.neuroimage.2011.10.018.

Power, J. D., Mitra, A., Laumann, T. O., Snyder, A. Z., Schlaggar, B. L., & Petersen, S. E. (2014). Methods to detect, characterize, and remove motion artifact in resting state fMRI. *Neuroimage, 84*(1), 320–341. https://doi.org/10.1016/j.neuroimage.2013.08.048.

Ram, R., Bromet, E. J., Eaton, W. W., Pato, C., & Schwartz, J. E. (1992). The natural course of schizophrenia: a review of first-admission studies. *Schizophr Bull, 18*(2), 185–207. https://doi.org/10.1093/schbul/18.2.185.

Rapoport, J. L., Giedd, J. N., & Gogtay, N. (2012). Neurodevelopmental model of schizophrenia: update 2012. *Molecular Psychiatry, 17*(12), 1228. https://doi.org/10.1038/mp.2012.23.

Reinen, J. M., Chén, O. Y., Hutchison, R. M., Yeo, B., Anderson, K. M., Sabuncu, M. R., & Baker, J. T. (2018). The human cortex possesses a reconfigurable dynamic network architecture that is disrupted in psychosis. *Nature Communications, 9*(1). https://doi.org/10.1038/s41467-018-03462-y.

Rizzolatti, G., & Sinigaglia, C. (2010). The functional role of the parieto-frontal mirror circuit: Interpretations and misinterpretations. *Nature Reviews Neuroscience, 11*(4), 264–274. https://doi.org/10.1038/nrn2805.

Rosanova, M., Casali, A., Bellina, V., Resta, F., Mariotti, M., & Massimini, M. (2009). Natural frequencies of human corticothalamic circuits. *Journal of Neuroscience the Official Journal of the Society for Neuroscience, 29*(24), 7679. https://doi.org/10.1523/JNEUROSCI.0445-09.2009.

Schölvinck, M. L., Maier, A., Ye, F. Q., Duyn, J. H., & Leopold, D. A. (2010). Neural basis of global resting-state fMRI activity. *Proc Natl Acad Sci U S A, 107*(22), 10238–10243. https://doi.org/10.1073/pnas.0913110107.

Siegel, M., Donner, T. H., & Engel, A. K. (2012). Spectral fingerprints of large-scale neuronal interactions. *Nature Reviews Neuroscience, 13*(2), 121–134. https://doi.org/10.1038/nrn3137.

Tang, J., Liao, Y., Song, M., Gao, J. H., Zhou, B., Tan, C., et al. (2013). Aberrant default mode functional connectivity in early onset schizophrenia. *PLoS One, 8*(7), e71061. https://doi.org/10.1371/journal.pone.0071061.

Thompson, P. M., Vidal, C., Giedd, J. N., Gochman, P., Blumenthal, J., Nicolson, R., & Rapoport, J. L. (2001). Mapping adolescent brain change reveals dynamic wave of accelerated gray matter loss in very early-onset schizophrenia. *Proceedings of the National Academy of Sciences of the United States of America, 98*(20), 11650–11655. https://doi.org/10.1073/pnas.201243998.

Thompson, W. H., & Fransson, P. (2015). The frequency dimension of fMRI dynamic connectivity: Network connectivity, functional hubs and integration in the resting brain. *Neuroimage, 121*, 227–242. https://doi.org/10.1016/j.neuroimage.2015.07.022.

van den Heuvel, M. P., & Fornito, A. (2014). Brain networks in schizophrenia. *Neuropsychol Rev, 24*(1), 32–48. https://doi.org/10.1007/s11065-014-9248-7.

van den Heuvel, M. P., & Hulshoff Pol, H. E. (2010). Exploring the brain network: a review on resting-state fMRI functional connectivity. *Eur Neuropsychopharmacol, 20*(8), 519–534. https://doi.org/10.1016/j.euroneuro.2010.03.008.

Wang, S., Zhang, Y., Lv, L., Wu, R., Fan, X., Zhao, J., & Guo, W. (2018a). Abnormal regional homogeneity as a potential imaging biomarker for adolescent-onset schizophrenia: A resting-state fMRI study and support vector machine analysis. *Schizophrenia Research.* https://doi.org/10.1016/j.schres.2017.05.038.

Wang, X., Liao, W., Han, S., Li, J., Zhang, Y., Zhao, J., & Chen, H. (2019). Altered dynamic global signal topography in antipsychotic-naive adolescents with early-onset schizophrenia. *Schizophrenia Research.* https://doi.org/10.1016/j.schres.2019.01.035.

Wang, X., Zhang, Y., Long, Z., Zheng, J., Zhang, Y., Han, S., & Zhao, J. (2017). Frequency-specific alteration of functional connectivity density in antipsychotic-naive adolescents with early-onset schizophrenia. *Journal of psychiatric research, 95*, 68–75. https://doi.org/10.1016/j.jpsychires.2017.07.014.

Wang, Y., Zhu, L., Zou, Q., Cui, Q., Liao, W., Duan, X., et al. (2018b). Frequency dependent hub role of the dorsal and ventral right anterior insula. *Neuroimage, 165*, 112–117. https://doi.org/10.1016/j.neuroimage.2017.10.004.

Wong, C. W., De Young, P. N., & Liu, T. T. (2016). Differences in the resting-state fMRI global signal amplitude between the eyes open and eyes closed states are related to changes in EEG vigilance. Neuroimage, 124, 24–31. https://doi.org/10.1016/j.neuroimage.2015.08.053

Wong, C. W., Olafsson, V., Tal, O., & Liu, T. T. (2013). The amplitude of the resting-state fMRI global signal is related to EEG vigilance measures. *Neuroimage, 83*, 983–990. https://doi.org/10.1016/j.neuroimage.2013.07.057.

Woo, C. W., Chang, L. J., Lindquist, M. A., & Wager, T. D. (2017). Building better biomarkers: brain models in translational neuroimaging. *Nature Neuroscience, 20*(3), 365–377. https://doi.org/10.1038/nn.4478.

Wu, C. W., Gu, H., Lu, H., Stein, E. A., Chen, J. H., & Yang, Y. (2008). Frequency specificity of functional connectivity in brain networks. *Neuroimage, 42*(3), 1047–1055. https://doi.org/10.1016/j.neuroimage.2008.05.035.

Wu, X., Wei, L., Wang, N., Hu, Z., Wang, L., Ma, J., & Shi, Y. (2016). Frequency of Spontaneous BOLD Signal Differences between Moderate and Late Preterm Newborns and Term Newborns. *Neurotoxicity Research*, 1–13. https://doi.org/10.1007/s12640-016-9642-4.

Yang, G. J., Murray, J. D., Glasser, M., Pearlson, G. D., Krystal, J. H., Schleifer, C., & Anticevic, A. (2016). Altered global signal topography in schizophrenia. *Cerebral Cortex, 27*(11), 5156–5169. https://doi.org/10.1093/cercor/bhw297.

Yang, G. J., Murray, J. D., Repovs, G., Cole, M. W., Savic, A., Glasser, M. F., & Pearlson, G. D. (2014). Altered global brain signal in schizophrenia. *Proceedings of the National Academy of Sciences of the United States of America, 111*(20), 7438–7443. https://doi.org/10.1073/pnas.1405289111.

Yu, R., Chien, Y. L., Wang, H. L. S., Liu, C. M., Liu, C. C., Hwang, T. J., & Seng, W. Y. I. (2014). Frequency-specific alternations in the amplitude of low-frequency fluctuations in schizophrenia. *Human Brain Mapping, 35*(2), 627–637. https://doi.org/10.1002/hbm.22203.

Yu, R., Ming, H. H., Wang, H. L. S., Liu, C. M., Liu, C. C., Hwang, T. J., & Tseng, W. Y. I. (2013). Frequency Dependent Alterations in Regional Homogeneity of Baseline Brain Activity in Schizophrenia. *Plos One, 8*(3), e57516. https://doi.org/10.1371/journal.pone.0057516.

Zhang, X., Yang, M., Du, X., Liao, W., Chen, D., Fan, F., & Chen, H. (2019). Glucose disturbances, cognitive deficits and white matter abnormalities in first-episode drug-naive schizophrenia. *Molecular Psychiatry.* https://doi.org/10.1038/s41380-019-0478-1.

Zheng, J., Zhang, Y., Guo, X., Duan, X., & Chen, H. (2015). Disrupted amplitude of low-frequency fluctuations in antipsychotic-naïve adolescents with early-onset schizophrenia. Psychiatry Res, 249. https://doi.org/10.1016/j.pscychresns.2015.11.006

Zhu, J., Cai, H., Yuan, Y., Yue, Y., Jiang, D., Chen, C.,Yu, Y. (2018). Variance of the global signal as a pretreatment predictor of

antidepressant treatment response in drug-naïve major depressive disorder. Brain Imaging & Behavior(Suppl 1), 1–7. https://doi.org/10.1007/s11682-018-9845-9

Zuo, X. N., Martino, A. D., Kelly, C., Shehzad, Z. E., Gee, D. G., Klein, D. F., & Milham, M. P. (2010). The oscillating brain: Complex and reliable. *Neuroimage, 49*(2), 1432. https://doi.org/10.1016/j.neuroimage.2009.09.037.